



Different shades of red: The complexity of mineralogical and physico-chemical factors influencing the colour of ceramics



Alberto De Bonis^{a,b,*}, Giuseppe Cultrone^c, Celestino Grifa^d, Alessio Langella^d, Antonio P. Leone^e, Mariano Mercurio^d, Vincenzo Morra^a

^a Dipartimento di Scienze della Terra, dell'Ambiente e delle Risorse (DiSTAR), Università degli Studi di Napoli Federico II, Complesso Universitario Monte S. Angelo, Via Cinthia 26, 80126 Napoli, Italy

^b Dipartimento di Strutture per l'Ingegneria e l'Architettura, Università degli Studi di Napoli Federico II, Via Claudio 21, 80125 Napoli, Italy

^c Departamento de Mineralogía y Petrología, Universidad de Granada, Avda. Fuentenueva s/n., 18002 Granada, Spain

^d Dipartimento di Scienze e Tecnologie, Università degli Studi del Sannio, Via dei Mulini 59/A, 82100 Benevento, Italy

^e Consiglio Nazionale delle Ricerche – Istituto per i Sistemi Agricoli e Forestali del Mediterraneo (CNR – ISAFoM), Via Patacca 85, 80056 Ercolano, NA, Italy

ARTICLE INFO

Keywords:

Ceramic colour
Experimental firing
Mineralogy
Colorimetry
Vis-NIR reflectance spectroscopy

ABSTRACT

Different techniques (X-ray diffraction, field emission scanning electron microscope, colorimetry, visible-near infrared reflectance spectroscopy) were carried out to investigate the cause of colour changes of traditional ceramic materials. Two clayey materials of different composition, collected in the Bay of Naples, were fired in oxidising atmosphere at different temperatures resulting in different shades of red colour.

Hematite is responsible of the reddish hue of ceramics and its nucleation is strictly related to firing temperature and chemical composition of the raw materials. A low CaO concentration allowed hematite to form in higher amounts providing a more intense reddish hue at high firing temperatures (over 950 °C). At the highest temperature (1100 °C) all samples showed darker colour due to increased size of iron oxide particles. Black core developed in Ca-rich ceramics fired at low temperatures as the short time of firing is insufficient to complete iron oxidation within the matrix, except in those containing high temper amounts. Indeed, microstructural modification occurs due to the presence of discontinuities among temper grains and matrix, which improves the circulation of oxygen in the core of ceramics.

1. Introduction

Bricks and other architectural ceramics have been used since ancient times for their low cost of production associated with optimal technological qualities, quite similar to those of natural stones. In the Bay of Naples, where volcanic stones represent the most common building material, ceramics were widely used for construction especially in Graeco-Roman times, along with a widespread production of pottery, with remarkable examples in the most important ancient settlements of this area, such as *Pompeii*, *Cumae*, *Puteoli*, *Stabiae*, and *Neapolis* [1–9]. More recently, bricks and other architectural terracottas (e.g., roof and floor tiles, water pipes, decorative elements) have played an essential role as building material in the historic city centres of the Bay of Naples area, having been used in combination with natural stones either as structural or decorative purposes [10,11].

A production of building ceramics of great economic importance in the Bay of Naples was that of the island of Ischia. The latter is

historically well known for the presence of both clayey materials and archaeological evidence of ceramic production dating back to the beginning of the Greek civilisation [6,12–15]. In the 16–17th centuries, and probably much earlier, bricks and floor tiles were widespread in the city of Naples, whereas terracotta pipes were used for water supply. The raw material from Ischia was also exported to be worked in the most important ceramic workshops of Naples, such as the *Ponte della Maddalena* factory producing the typical majolica tiles (*riggiolate*) of Naples [12]. Ceramic production and clay exploiting in the island lasted until the early 20th century and no longer exist today [12].

Another example of production of ceramics in the Bay of Naples area is on the Sorrento Peninsula, where a long lasting traditional manufacture exploiting local raw materials is still active today. Bricks produced there are renowned for their refractory properties and are mainly used to build wood-burning ovens for cooking food, bread and pizza in particular [14,15].

Bricks and architectural terracotta have always played a key role in

* Corresponding author at: Dipartimento di Scienze della Terra, dell'Ambiente e delle Risorse (DiSTAR), Università degli Studi di Napoli Federico II, Complesso Universitario Monte S. Angelo, Via Cinthia 26, 80126 Napoli, Italy.

E-mail address: alberto.debonis@unina.it (A. De Bonis).

<http://dx.doi.org/10.1016/j.ceramint.2017.03.127>

Received 21 February 2017; Received in revised form 19 March 2017; Accepted 20 March 2017

Available online 22 March 2017

0272-8842/ © 2017 Elsevier Ltd and Techna Group S.r.l. All rights reserved.

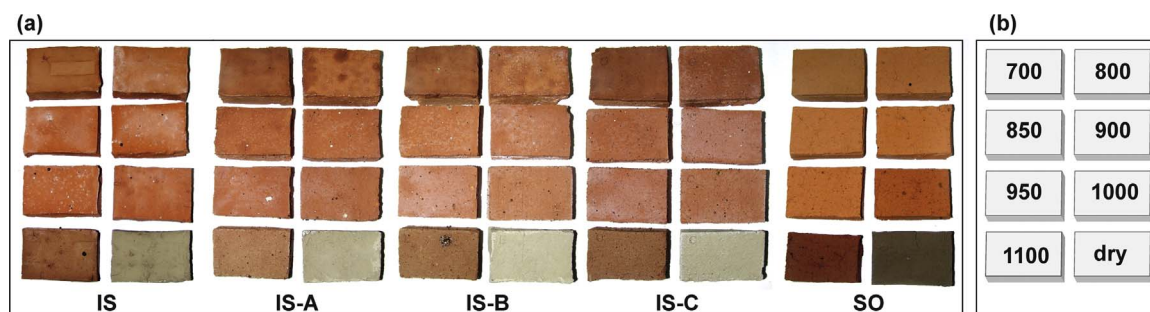


Fig. 1. (a) Image showing the test pieces and (b) the arrangement of samples fired at different temperatures (°C) and unfired (dry). Legend: IS=Island of Ischia; SO=Sorrento Peninsula; percentage of temper added in IS samples is indicated by the following labels: IS-A=10%; IS-B=20%; IS-C=30%. (For interpretation of the references to colour in this figure, the reader is referred to the web version of this article.)

the “urban colouring” due to their aesthetic appeal. Colour of ceramics is achieved through complicated mineralogical and chemical reactions during the firing process, which depend on the raw material composition and firing dynamics, such as oxidising/reducing conditions of kiln atmosphere, temperature, and time [16,17]. Due to the complexity of these factors, architectural ceramics can exhibit a variety of natural and pleasant warm colours. This is particularly true whenever traditional and ancient ceramics are concerned, where effects such as shaded surfaces and black core are typical and can be considered as peculiarities that strongly mark the differences with the modern and standardised industrial products. Hence, colour is an important aspect to take into account when replacing damaged bricks or tiles is required for restoration of the historical/archaeological buildings [18].

The main objective of this study is the investigation of colour changes in ceramics made with two different types of clayey raw materials from the Bay of Naples area, collected in the island of Ischia and in the Sorrento Peninsula respectively, with particular attention to archaeological and traditional ceramics. For this purpose, ceramic replicas were made via experimental firing in order to simulate a traditional production process and reproduce the aesthetic and technological features of ancient ceramics. Different methods were applied to analyse colour and mineralogical changes occurring during firing in ceramics made with different raw materials. This can be useful for manufacturing replacement ceramic building materials with the most suitable characteristics for use in restoration work. Moreover, the quantitative assessment of colour can also be suited for archaeological purposes, as colour of ceramics is one of the main macroscopic features used to describe pottery and obtain a preliminary evaluation of firing dynamics [16,19].

2. Experimental

2.1. Materials

Ceramic replicas and raw materials have been characterised through deep mineralogical, chemical, petrophysical, and microstructural analyses in order to investigate the technological features of ceramic materials produced with different raw materials and mix design. Details concerning this investigation are given in De Bonis et al. [14,15]. There follows a summary of these results.

2.1.1. Raw materials

The mix design for the ceramic replicas has been made considering the chemical composition and petrographic features of archaeological and traditional ceramics from the Bay of Naples and other regional sites, acquired from previous studies, which evidenced the use of clays with different composition and volcanic temper as a function of their final use [1,3–6,8,9,20–22]. One of the two clayey raw materials used for the ceramic replicas is a Ca-poor (CaO=2.57 wt%) reworked weathered pyroclastics from the Sorrento Peninsula (hereafter SO), mostly composed of volcanic minerals (feldspar, pyroxene), along with

quartz, and clay minerals (illite/mica and dehydrated halloysite) [14,15] (Fig. 2a). The other raw material is a Ca-rich (CaO=9.70 wt %) marine sediment from the island of Ischia (hereafter IS) containing quartz, feldspar, calcite, minor dolomite and different clay minerals, such as illite/mica, kaolinite, chlorite, and illite-smectite mixed-layer [14,15] (Fig. 2b).

The organic matter in the two raw materials is 5.95 wt% (IS) and 7.59 wt% (SO). The temper is a volcanic sand of trachytic composition from the Campi Flegrei area [14,15]. Four types of clay bodies were manufactured with IS clay. The first type was prepared without any temper addition (IS), while the other three types were clay/temper mixtures prepared with 10% (IS-A), 20% (IS-B), and 30% (IS-C) in weight of temper. The SO clay body was prepared without any temper addition, owing to the natural abundance of coarse inclusions with a predominantly volcanic origin.

2.1.2. Ceramic replicas

The clay bodies were moulded with a brick shape of ca. 32×24×4 cm in size and then fired at seven different temperatures (700, 800, 850, 900, 950, 1000 and 1100 °C) (Fig. 1) in oxidising atmosphere in an electric furnace (Nabertherm HTCT 08/16) equipped with an electronic controller (Nabertherm P330). Firing time depended on the selected temperature and ranged from a minimum of 5 h 40 min (700 °C) to 7 h 40 min (1100 °C), in relation to a fixed firing curve characterised by a slow initial heating rate (1.5 °C min⁻¹), followed by a higher heating rate (3 °C min⁻¹) starting from 200 °C up to the maximum *T*, 90 min soaking time and then by cooling. These conditions are usually adopted in the current traditional wood-firing productions in the Bay of Naples.

The ceramic replicas showed different technological properties depending on the raw materials composition, mix-design, and firing dynamics (temperature and time). Indeed, structural and mineralogical transformations occurred with firing. De Bonis et al. [15] evidenced that in Ca-rich (IS) samples, starting from approximately 850 °C, calcite reacted with clay minerals forming Ca-silicates such as melilite (gehlenite) and pyroxene (Al-rich diopside) [15,23,24]; newly forming Ca-plagioclase feldspar (anorthite) was also detected at the maximum *T* (1100 °C) [15,23] (Fig. 2b). Small amounts of calcite resisted up to temperatures higher than that expected (~850 °C) (Fig. 2b). This could be due both to a relatively short firing duration and to the presence of coarse calcite grains [15]. Hematite appeared at 700 °C following iron oxidation (Fig. 2b). In Ca-poor (SO) replicas pyroxene is present as primary phase and the only newly formed minerals are represented by high amounts of hematite, increasing with firing *T*, and mullite at 1100 °C (Fig. 2a). In Ca-rich (IS) replicas the crystalline framework created by newly formed Ca-silicates, associated to extensive vitrification, produced a well-sintered and hard microstructure already starting from 850 °C. This structure is characterised by lower water absorption compared to Ca-poor (SO) replicas, which show a poorly sintered and more porous microstructure up to 1000 °C. At maximum *T* (1100 °C) both IS and SO ceramics are characterised by hard bodies due to

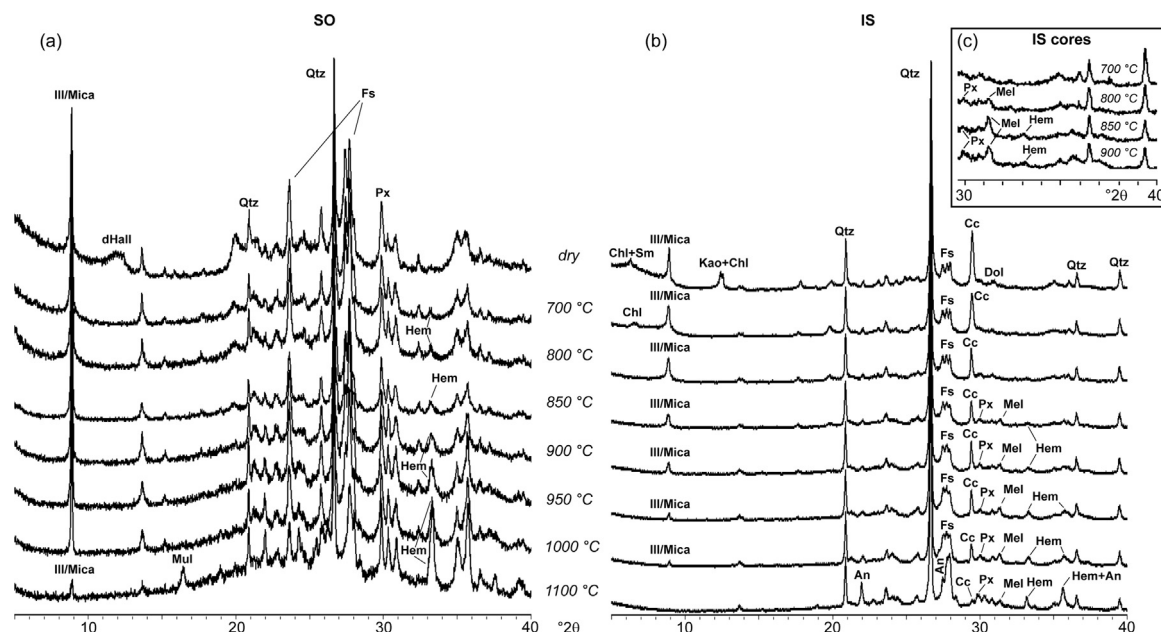


Fig. 2. XRPD patterns of unfired (dry) and fired SO (a) and IS (b) samples. The patterns of the IS cores from 700 to 900 °C were reported in the inset (c). Mineral abbreviations: Qtz, quartz; Fs, feldspar; Cc, calcite; Dol, dolomite; Px, pyroxene; Mel, melilite; An, anorthite; Hem, hematite; Mul, mullite; Ill, illite; Sm, smectite; Kao, kaolinite; Chl, chlorite; dHall, dehydrated halloysite. Bricks abbreviations are indicated in Fig. 1.

continuous vitrification, which determines the formation of unconnected porosity and low water absorption. Coarse grains of temper added to IS replicas determined the formation of a porosity represented by discontinuities at temper/matrix interfaces, which slightly increase water absorption when temper amount is high (20–30 wt%) and also cause dissipation of elastic energy, improving the toughness of the ceramics (i.e., when ceramics are used on fire or transported) [15].

2.2. Methods

Mineralogical and microstructural information on ceramic replicas was obtained by X-ray powder diffraction (XRPD) and field emission scanning electron microscope coupled with energy dispersive spectroscopy microanalysis (FESEM-EDS). These techniques, although relevant and practically irreplaceable for detailed mineralogical investigation are, however, costly and time-consuming. For that, other fast and less expensive technique should be considered. Among these, reflectance spectroscopy in the visible-near infrared (vis-NIR RS, 350–2500 nm) spectral domain could result very profitable. This technique has been successfully applied to characterise soil compounds (organic carbon, clay minerals, iron oxides) [25–27], while in archaeometry it was only used for the study of painting [28–30] and, even more rarely on ceramics, where was only limited to the analysis of decoration and glaze [31,32]. Colour of ceramic replicas was quantitatively evaluated by portable colorimetry in CIE $L^* a^* b^*$ colour space coordinates. This approach has largely been used for the determination of archaeological ceramics [9,16,33–35]. Colour was also qualitatively assessed via visual inspection using the Munsell Soil Colour Chart as commonly performed by archaeologists and also in several archaeometric studies [1,4–6,36,37]. This could be very useful to quickly check the colour changes of ceramic bodies at each firing temperature. An alternative method for the determination of the colour of ceramic samples could be based on the transformation of the visible (350–780 nm) spectral reflectance, which can be converted to both CIE $L^* a^* b^*$ and Munsell notations. As above, this approach has already been used in mineralogical studies, but never, at least according to our information, in those regarding ceramics. For that, it has been used in the present study and their result has been compared with those derived from traditional colorimetry.

2.2.1. Mineralogical and microstructural analyses

Mineralogical analyses were performed on different coloured parts of the ceramic replicas via X-ray powder diffraction (XRPD) with a PANalytical X'Pert PRO 3040/60 PW diffractometer (CuK α radiation, 40 kV, 40 mA, scanning interval 4–50° 2 θ , equivalent step size 0.017° 2 θ , equivalent counting time 15.5 s per step, RTMS X'Celerator detector). Microchemical analyses of mineral phases and microstructural observation were performed using a Leo Gemini 1530 high resolution field emission scanning electron microscope (FESEM) coupled with an Oxford Inca 200 energy dispersive spectroscopy (EDS) microanalysis.

2.2.2. Portable colorimetry

A portable Minolta CM700d spectrophotometer was used to determine the chromatic coordinates of unfired and fired samples. Compared to a common tristimulus colorimeter, Minolta CM700d instrument has a higher precision and it is suitable for complex colour analysis as it can determine the spectral reflectance in the visible wavelength range (400–700 nm). Colour space coordinates CIE $L^* a^* b^*$ with an illuminant C, which simulated daylight with a colour temperature of 6774 K were determined (8° view angle, 10° observer). A pulsed xenon lamp with UV cut filter illuminated the surface of the sample with a spot size of 3 mm in diameter, and a silicon photodiode array detected and measured both incident and reflected light.

2.2.3. Vis-NIR reflectance spectroscopy

Diffuse visible-near infrared (vis-NIR) reflectance spectroscopy is another non-destructive technique we used to perform spectroscopic analysis of unfired samples and ceramic replicas, trying to acquire useful data for the characterisation of building and archaeological ceramics. This technique is based on the interaction of light with matter in the visible-near infrared (350–2500 nm) spectral domain, which involves vibrational and electronic transition in the investigated material [38]. The radiance over the ceramic samples was measured with an ASD FieldSpec 350–2500 pro nm spectroradiometer (Analytical Spectral Devices Inc., Boulder, Colorado, USA), and converted to spectral reflectance by dividing the radiance of target by the one of a standard white reference plate ('spectralon'), measured under the same conditions of illumination. Samples were illuminated with a

Table 1

Colour coordinates (CIE $L^* a^* b^*$, illuminant C) of unfired and fired ceramics, acquired with both portable colorimetry and vis-NIR techniques. Munsell colour notations obtained from vis-NIR data and from visual inspection (Munsell soil colour chart) were also reported. Bricks abbreviations are indicated in Fig. 1.

Sample	Point	Colour coordinates						Munsell colour notations	
		Portable colorimetry			Vis-NIR reflectance			Vis-NIR reflectance	Visual inspection (Munsell soil colour chart)
		L^*	a^*	b^*	L^*	a^*	b^*		
IS dry		54.59	2.89	16.72	71.41	0.85	13.47	1.35Y 6.98/1.93	2.5Y 6/3 (light yellowish brown)
IS 700c	Core	39.51	0.28	3.95	37.41	0.06	1.65	3.20Y 3.68/0.24	Gley 1 4/N (dark grey)
IS 700e	Margin	56.61	13.50	25.21	57.07	12.05	23.29	5.53YR 5.60/4.66	7.5YR 6/6 (reddish yellow)
IS 800c	Core	46.90	0.99	8.21	45.61	0.47	5.21	2.27Y 4.47/0.76	4Y 4/2 (olive grey)
IS 800e	Margin	61.43	14.40	27.61	54.30	13.45	24.66	5.01YR 5.33/4.91	7.5YR 6/6 (reddish yellow)
IS 850c	Core	54.60	2.95	12.85	50.46	1.91	8.62	0.08Y 4.95/1.37	2.5Y 5/2 (greyish brown)
IS 850e	Margin	62.19	16.52	29.29	59.86	14.04	25.14	4.65YR 5.88/5.11	7.5YR 6/6 (reddish yellow)
IS 900c	Core	60.27	12.29	28.21	55.46	10.35	23.05	6.44YR 5.44/4.31	7.5YR 6/4 (light brown)
IS 900e	Margin	61.38	18.34	30.06	53.29	16.29	27.03	4.26YR 5.23/5.58	5YR 6/6 (reddish yellow)
IS 950		60.93	18.92	28.26	59.08	14.59	26.38	4.71YR 5.80/5.32	5YR 6/6 (reddish yellow)
IS 1000		59.83	15.44	23.11	55.77	13.42	21.07	3.89YR 5.47/4.52	5YR 5/6 (yellowish red)
IS 1100		53.99	13.95	19.40	49.42	10.63	15.46	3.73YR 4.84/3.38	5YR 5/4 (reddish brown)
IS-A dry		52.15	3.50	18.71	71.25	0.69	12.71	1.50Y 6.96/1.81	2.5Y 6/3 (light yellowish brown)
IS-A 700c	Core	44.01	0.71	6.75	41.70	0.19	3.85	3.01Y 4.09/0.54	7.5Y 4/1 (grey)
IS-A 700e	Margin	53.21	14.15	24.10	57.67	11.44	25.25	6.29YR 5.66/4.75	7.5YR 6/6 (reddish yellow)
IS-A 800c	Core	47.45	0.50	6.92	48.97	0.32	6.40	2.81Y 4.80/0.93	7Y 5/1 (grey)
IS-A 800e	Margin	52.04	17.73	26.88	60.76	10.85	24.37	6.32YR 5.97/4.59	5YR 5/5 (yellowish red)
IS-A 850c	Core	52.54	1.39	8.53	48.65	0.62	5.75	1.91Y 4.77/0.85	5Y 6/1 (grey)
IS-A 850e	Margin	61.25	15.06	27.43	57.67	10.89	21.70	5.58YR 5.66/4.24	7.5YR 6/6 (reddish yellow)
IS-A 900c	Core	56.77	6.03	18.31	49.82	3.76	12.15	8.81YR 4.88/2.05	2.5Y 5/3 (light olive brown)
IS-A 900e	Margin	60.48	16.25	28.54	54.52	16.69	22.45	4.23YR 5.35/4.70	5YR 6/6 (reddish yellow)
IS-A 950		60.42	17.56	27.22	59.64	14.10	25.01	4.59YR 5.86/5.10	5YR 6/6 (reddish yellow)
IS-A 1000		57.01	18.58	26.22	50.28	15.77	24.19	3.86YR 4.93/5.14	5YR 5/6 (yellowish red)
IS-A 1100		54.25	11.87	17.61	51.78	11.65	19.00	4.30YR 5.08/3.99	5YR 5/4 (reddish brown)
IS-B dry		54.66	3.01	17.92	70.49	0.85	12.74	1.34Y 6.89/1.83	2.5Y 5/3 (light olive brown)
IS-B 700c	Core	47.72	0.74	7.27	41.06	-0.01	4.44	3.83Y 4.03/0.62	7.5Y 5/1 (grey)
IS-B 700e	Margin	59.45	10.64	24.76	56.35	8.49	21.99	7.51YR 5.53/3.94	10YR 6/6 (brownish yellow)
IS-B 800c	Core	55.18	2.68	13.95	49.24	1.51	10.97	1.36Y 4.83/1.66	2.5Y 5/2 (grayish brown)
IS-B 800e	Margin	58.70	14.26	27.28	56.90	10.40	22.96	6.34YR 5.58/4.32	7.5YR 6/6 (reddish yellow)
IS-B 850		58.59	16.55	26.19	53.42	10.64	23.21	6.37YR 5.24/4.35	5YR 6/6 (reddish yellow)
IS-B 900		58.70	17.96	28.97	55.32	13.87	25.03	4.85YR 5.43/5.02	5YR 6/6 (reddish yellow)
IS-B 950		61.37	14.96	24.86	58.81	15.12	25.36	4.20YR 5.77/5.29	5YR 6/6 (reddish yellow)
IS-B 1000		56.37	16.07	23.72	58.56	13.80	21.77	3.83YR 5.75/4.69	5YR 5/6 (yellowish red)
IS-B 1100		53.11	10.87	16.58	54.13	10.14	16.76	4.42YR 5.31/3.51	7.5YR 5/4 (brown)
IS-C dry		51.60	3.34	17.76	73.41	0.92	14.48	1.29Y 7.19/2.08	2.5Y 5/3 (light olive brown)
IS-C 700		58.83	10.48	24.01	59.32	8.89	23.64	7.55YR 5.83/4.22	10YR 6/4 (light yellowish brown)
IS-C 800		58.79	13.18	24.85	57.65	10.81	23.40	6.16YR 5.66/4.44	7.5YR 6/6 (reddish yellow)
IS-C 850		60.04	15.84	23.56	56.31	14.88	24.17	4.10YR 5.46/5.04	5YR 6/6 (reddish yellow)
IS-C 900		55.50	17.53	25.36	60.98	11.67	23.26	5.47YR 5.93/4.52	5YR 6/6 (reddish yellow)
IS-C 950		53.89	17.29	25.46	56.52	11.25	18.33	4.21YR 5.49/3.85	5YR 6/6 (reddish yellow)
IS-C 1000		53.30	17.83	25.73	54.72	13.55	19.55	3.36YR 5.31/4.32	5YR 5/6 (yellowish red)
IS-C 1100		51.91	9.95	20.40	51.95	10.04	15.88	4.23YR 5.04/3.35	7.5YR 5/4 (brown)
SO dry		41.00	5.12	15.68	57.66	2.44	12.33	0.04Y 5.60/1.91	10YR 4/2 (dark greyish brown)
SO 700		64.84	10.56	26.23	59.11	10.38	23.23	6.37YR 5.81/4.37	7.5YR 7/4 (pink)
SO 800		61.13	15.33	29.36	60.44	8.99	21.51	6.80YR 5.94/3.98	7.5YR 6/6 (reddish yellow)
SO 850		60.96	16.88	31.35	62.43	11.62	25.27	6.00YR 6.14/4.82	7.5YR 6/6 (reddish yellow)
SO 900		60.94	18.19	31.97	62.81	12.54	27.43	5.99YR 6.18/5.21	7.5YR 6/6 (reddish yellow)
SO 950		56.83	20.01	31.82	57.74	16.29	29.02	4.58YR 5.67/5.86	5YR 6/6 (reddish yellow)
SO 1000		52.19	21.35	30.73	55.70	16.72	28.94	4.45YR 5.46/5.89	5YR 5/8 (yellowish red)
SO 1100		44.27	18.59	23.46	44.12	13.92	8.52	3.92YR 4.28/4.24	2.5YR 3/6 (dark red)

70 W quartz-tungsten-halogen light under a 30° illumination angle. Spectral measurements were made at the nadir, i.e. the sensor viewing vertically. The distance between the spectroradiometer and the sample was about 3 cm, allowing radiance measurements of a circular area of ca. 1.2 cm diameter. To reduce instrumental noise, four measurements recorded for each sample were averaged. Average reflectance spectra were filtered using the Savitzky-Golay algorithm [39], in order to reduce the high-frequency instrumental noise, then transformed into their absorbance spectra ($A = \log(1/R)$), from which second derivative curves were calculated using the software SpecPro [40]. The position of absorption bands was identified on the second derivative curves and

their amplitude was calculated [25,38] with the software SPEX (Spectral Explorer) [41].

The original spectral curves were resampled between 370 and 780 nm (visible domain) and transformed into the X, Y, and Z tristimulus values according to the Commission Internationale de l'Eclairage (CIE, 1931) using SpecPro [40]. Tristimulus values were then converted to Munsell (hue, value, chroma) and CIE $L^* a^* b^*$ colour notations, using the Munsell Conversion Program (version 12.15.1d; <http://wallkillcolor.com/>).

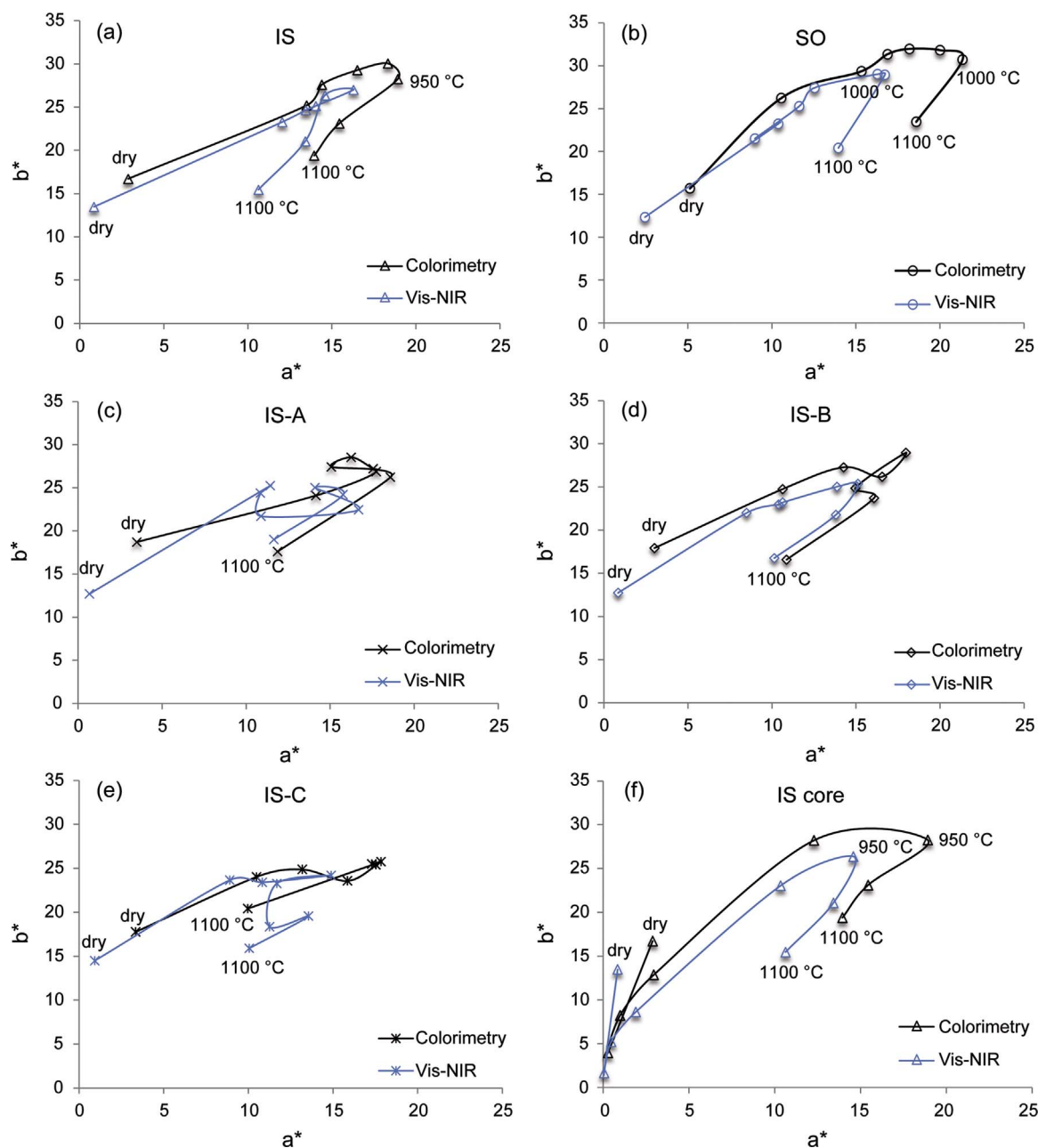


Fig. 3. Plot of colour coordinates (a^* , b^*) of unfired (dry) and fired samples of IS and SO ceramic replicas. Colours of both portable colorimetry and vis-NIR techniques were reported for comparison. Bricks abbreviations are indicated in Fig. 1. (For interpretation of the references to colour in this figure legend, the reader is referred to the web version of this article.)

2.2.4. Statistical analysis

Principal component analysis (PCA) [42] was alternatively applied to Munsell colour notations and the depth of absorption bands on the second derivative using XLSTAT (Addinsoft™) for statistical analysis. In the context of spectral data analysis, PCA has been successfully applied by many authors (e.g., Leone and Sommer [43] and references therein). Using this approach, the original spectral variables (e.g., spectral bands or colour notations) are replaced by a smaller number of uncorrelated variables, which account for the greatest possible proportion of the total variability. The principal components represent a new reference system where samples are characterised by a limited set of coordinates (e.g., one for each principal component) [43].

To establish the physical significance of the principal components, it is common practice to look at the relationships between the original variables and the eigenvectors, commonly referred to as factor loadings [44]. The original variables having large loadings on a given principal component, determine its physical significance. The position of sam-

ples in the new reference system of principal components can be used to identify groups of similar samples. In this study we have used PCA to identify groups of ceramics according to their spectral characteristics.

3. Results and discussion

3.1. Analysis of colour

Colour changes occurred in ceramic replicas mostly depending on temperature and mix design. Table 1 reports the CIE (L^* , a^* , b^*) colour coordinates for unfired and fired samples, along with Munsell colour notations obtained from vis-NIR reflectance and visual inspection respectively. Variation of colour saturation coordinates (a^* , b^*) is shown in binary diagrams (Fig. 3), where curves obtained by both portable colorimetry and vis-NIR reflectance data in the visible domain are compared. It is worth to note that both techniques provided curves with similar trends and that differences are generally due to higher a^*

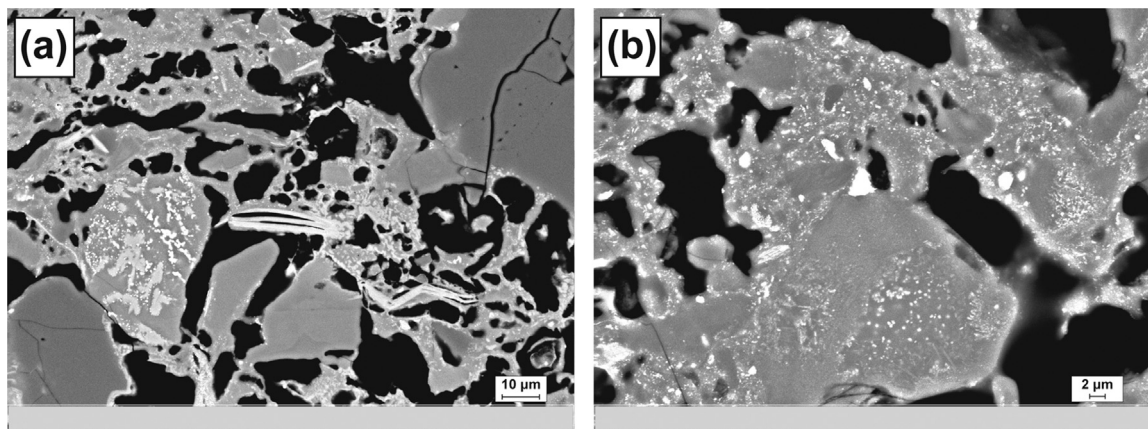


Fig. 4. Backscattered electrons FESEM images of samples (a) IS-C-1100 and (b) SO 1100, showing iron oxides particles (white dots) in the amorphous phase. Bricks abbreviations are indicated in Fig. 1.

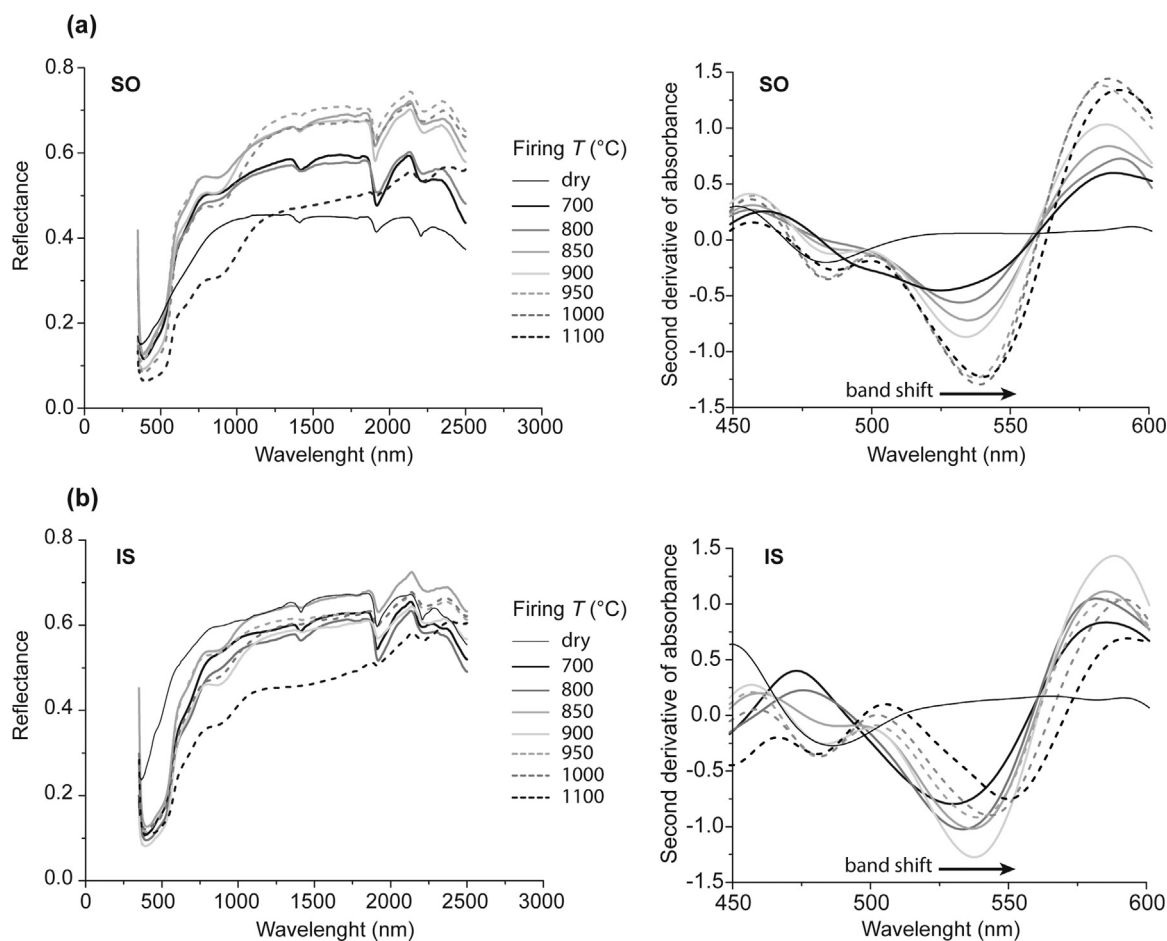


Fig. 5. Reflectance spectra (left) of (a) SO and (b) IS replicas, along with plots of second derivative of absorbance (right) in the region from 450 to 600 nm showing band shift with firing temperature. Bricks abbreviations are indicated in Fig. 1.

and b^* values of portable colorimetry (Fig. 3).

The unfired clay bodies are characterised by brownish colours in part due to the presence of organic matter, which reaches 5.95 wt% in IS clay and 7.59 wt% in SO clay, as reported in De Bonis et al. [15]. Increase of colour saturation (Table 1 and Fig. 3), corresponding to the intensity of the red hue, occurred during firing in all ceramic replicas due to the formation of hematite (Fig. 2a–c). At maximum T (1100 °C) a marked decrease of colour saturation occurs and all ceramic replicas showed darker hues (Fig. 1a). This inverse trend of colour saturation in IS samples already started at lower T (ca. 900 °C) (Fig. 3a). As reported

in literature [16,17,45,46], hematite formation in Ca-rich ceramics is limited by the development of newly formed Ca-silicates (e.g., pyroxene, melilite) (Fig. 2b), which incorporate Fe^{3+} in their framework around 900 and 1000 °C. These combined effects can explain the inverse trend of colour saturation at lower T in IS ceramics.

On the contrary, in Ca-poor SO replicas, owing to the absence of newly formed Ca-silicates, higher hematite amounts can develop consistently with firing up to maximum T (1100 °C) (Fig. 2a), although colour saturation decreases (Fig. 3b) producing a strong dark red hue (Fig. 1). At maximum T (1100 °C) colour of IS ceramics turn darker as



Fig. 6. Black core in sample IS-A fired at 700 °C. Bricks abbreviations are indicated in Fig. 1.

well assuming a reddish brown hue. At this T the amount of iron in the structure of some minerals (i.e., Ca-silicates) diminishes following their breakdown and is available for further development of hematite, which will be hosted in the glassy phase [46].

Darkening occurring at maximum T in both IS and SO ceramics is likely related to the presence of sub-micrometric iron oxide particles located in the glassy phase, which become larger and visible at FESEM (Fig. 4a and b) and that are attributable to hematite [46]. According to some authors, particle size of iron oxides is a primary source of colour differences in the same material, becoming darker as particle size increases [31,47]. Opuhovic and Kareiva [31] demonstrated that increasing annealing temperature of Fe^{3+} oxide-based pigments, a dark red hue developed due to increase of crystallite size. In these pigments, absorption bands in the region from 400 to 600 nm visibly shift to longer wavelength by increasing annealing temperature [31]. Actually, in SO replicas a progressive shift of bands from approximately 525 (700 °C) to 540 (1100 °C) nm, attributable to hematite, was recorded (Fig. 5a). In IS replicas, hematite band shift in this region is clearly visible from 700 to 800 °C, then it decreases at intermediate T due to the formation of Ca-silicates, and then it increases again only starting from 1000 °C (Fig. 5b) for further growth of hematite.

As far as tempered replicas are concerned, colour curves show a similar trend, but irregular patterns (Fig. 3c–e), probably for the presence of temper grains determining a less homogeneous colour of sample surfaces.

Another interesting chromatic feature concerns the formation of a blackish hue in the interior of IS ceramics fired at low temperatures (Fig. 6), which show low a^* values (Fig. 3f). These blackish hues,

known in ceramic terminology as black core, gradually faded away as T increased (Fig. 7). This is due to the shorter firing duration at low temperatures, which was not sufficient for the complete oxidation within the ceramic body thus reducing the hematite formation (Fig. 2c). At higher temperatures longer firing duration allowed oxygen to completely oxidise carbon to CO_2 and form hematite, turning the whole ceramic body to red [48,49].

Actually, presence of black core also depends on temper amount. Indeed, considering the same firing temperatures, IS replicas showed a vanishing of black core as temper amount increases, being totally absent with the maximum temper amount (Fig. 7). In this case, microstructural modification occurs due to the presence of discontinuities at the grain/matrix boundary [15]. The increased porosity allows oxygen to easily reach the interior of ceramics, also permitting the leakage of the reducing gases (CO , CO_2) released by the combustion of the organic matter and decarbonation of carbonates [49,50]. For this reason the higher porosity of SO ceramics completely prevented the black core formation (Fig. 7).

As far as Munsell colour notations are concerned, data measured via vis-NIR reflectance are more precise and detailed compared to those acquired via visual inspection on constant-hue charts (Table 1). Indeed, visual comparisons are unavoidable subjective and are prone to errors associated with differences in colour perception between individuals and the effects of variations in illumination conditions [51]. However, major colour differences, related to firing temperature and composition, are also distinguished by visual comparison.

3.2. Principal component analysis of vis-NIR spectral reflectance data

Results of PCA applied to the hue, value and chroma Munsell notations showed that the first two principal components accounted for 97.52% of the observed variance. The first and second PCs accounted, respectively for 67.25% and 30.26% of the total variation of the initial colour variables. These two components were then retained for the interpretation of relationships between ceramic samples.

In the plot of the first two principal components (Fig. 8a) three groups of ceramic samples can be clearly observed: two groups enclosing all the IS unfired bricks (C1) and black cores (C2), and a third group (C3) enclosing all the other samples (Fig. 8a). The ceramic group C1 is separated from the other groups along the second axis. A relatively large contribution to this axis derives from value. Groups C2 and C3 are separated from each other along the first axis, which is positively related to chroma and negatively to hue (Fig. 8a).

PCA applied to the depth absorption bands showed a clear

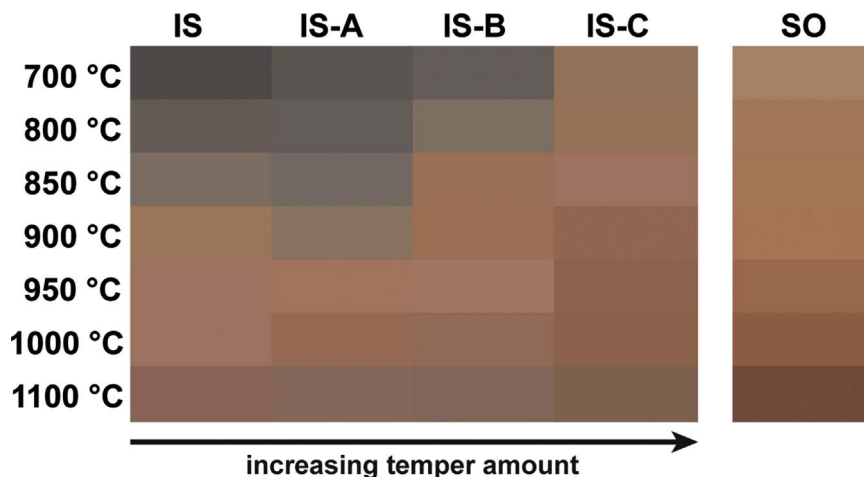


Fig. 7. Colour changes measured via portable colorimetry in the cores of the ceramic replicas. Bricks abbreviations are indicated in Fig. 1. (For interpretation of the references to colour in this figure legend, the reader is referred to the web version of this article.)

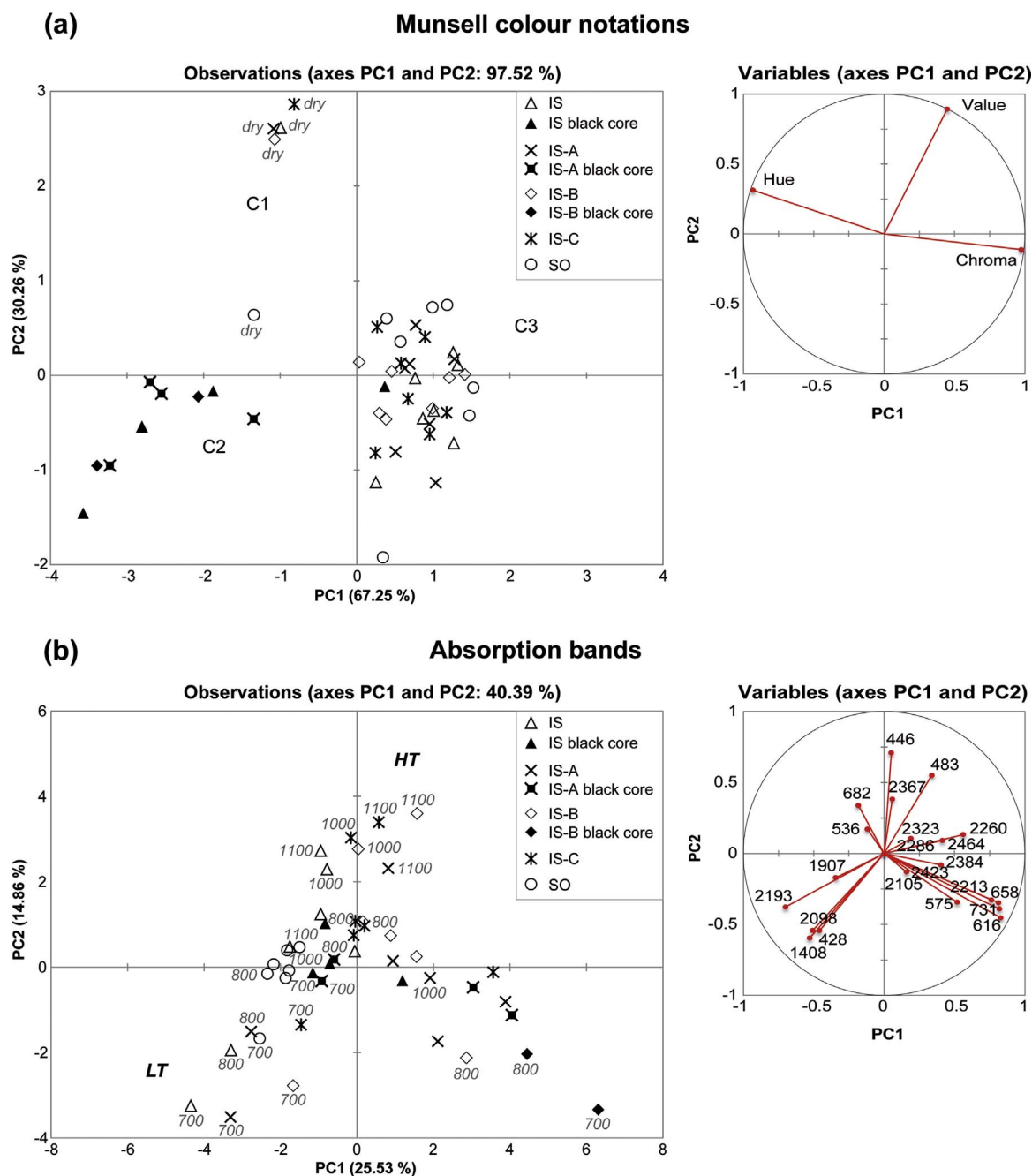


Fig. 8. Scatterplot of samples and variables on the plane defined by the first two principal components resulting from the application of PCA to vis-NIR reflectance data of Munsell colour notations (a) and absorption bands (b). Bricks abbreviations are indicated in Fig. 1.

separation between unfired and fired samples (plot not shown). Then we applied PCA only to fired samples in order to discriminate more in detail the effects of the heating process.

Results of PCA applied to the depth of absorption bands of fired ceramic samples showed the first two components explained 40.39% of the initial variation of these variables. PC1 and PC2 explained, respectively, 25.53% and 14.86% of the observed variance of the original data-set. Much of the remaining information is explained by the remaining principal component. However, the analysis of the distribution of ceramic samples in the plots of pairs of these components does not show relevant information. Therefore, only the plot of the first two principal components was considered for the interpretation of relationships among fired ceramic samples on the basis of the depths of absorption bands.

As shown in Fig. 8b, we can broadly distinguish samples fired at T

below 800 °C (LT) from those fired at T over 1000 °C (HT). Separation of LT samples mainly occurs at negative values on F1 and F2 axes, and is likely due to the absorption bands (1400–1900 nm) related to residual molecular water in clay phases [52–54]. SO samples fired above 800 °C mainly cluster along the negative F1 axis probably for the contribution of hematite bands at ca. 530 nm (Fig. 8b), whereas most black core samples are grouped closer to zero along the two axes. Other samples mostly scatter along the first axis, positively related to bands peaks near 2200, 2300 and 2400 nm attributed to Al–OH bend plus O–H stretch combinations (i.e., phyllosilicates) and bands possibly related to calcium carbonate (~2350 nm) [54]; a contribution to this axis is also given by bands from approximately 570 to 730 nm in the iron oxides region [38,47].

4. Conclusive remarks

The experimental tests on ceramic replicas from the Bay of Naples showed that their colour and durability depend on the raw material composition, firing dynamics, and mix design.

Fired replicas showed different shades of red, which triggered the formation of hematite from oxidation of free iron in oxidising firing atmosphere. In Ca-poor ceramics from the Sorrento Peninsula red hues become more intense as firing temperature increases for the formation of high hematite amounts. On the contrary Ca-rich ceramics from the Island of Ischia are characterised by an increase of red hue only up to ca. 900 °C. At higher temperatures a decrease of colour saturation occurred in Ischia samples due to the formation of calcium silicates (melilite and pyroxene), which hindered the hematite formation. At maximum temperature colour of all ceramic replicas turned to darker reddish hues. Darkening is probably related to the formation of large particles of hematite dispersed in the glassy phase formed at this temperature.

A black core formed in the Ischia ceramics fired at low temperatures. This is due to the short firing duration and low temperatures that did not allow the complete oxidation within the ceramic body. The black core gradually fades away as temperature increased. It is interesting to note that the increase of temper amount limited the formation of a black core due to discontinuities at grain/matrix boundary, which provided gas drainage paths during firing.

Acknowledgements

This work was supported by the following grants: V.M. (LR 5/02 2008, 04-C00001720), C.G. (LR 5/02 2008, 04-A00001703), from the Dipartimento di Scienze della Terra, dell'Ambiente e delle Risorse (DiSTAR) of the Università degli Studi di Napoli Federico II (V.M.), from the research project MAT2016-75889-R of the Spanish Government and the Research Group RNM179 of the Junta de Andalucía. The authors wish to thank Dr. Fulvio Fragnito, CNR-ISAFO, for its valuable assistance in the acquisition phase of spectroradiometric measurement.

References

- [1] V. Morra, A. De Bonis, C. Grifa, A. Langella, L. Cavassa, R. Piovesan, Mineropetrographic study of cooking ware and Pompeian red ware (Rosso Pompeiano) from Cuma (Southern Italy), *Archaeometry* 55 (2013) 852–879. <http://dx.doi.org/10.1111/j.1475-4754.2012.00710.x>.
- [2] C. Grifa, A. Langella, V. Morra, G. Soricelli, Pantellerian ware from Miseno (Campi Flegrei, Naples), *Period. Mineral.* 74 (2005) 69–86.
- [3] C. Grifa, V. Morra, A. Langella, P. Munzi, Byzantine ceramic production from Cuma (Campi Flegrei, Napoli), *Archaeometry* 51 (2009) 75–94. <http://dx.doi.org/10.1111/j.1475-4754.2008.00416.x>.
- [4] C. Grifa, A. De Bonis, A. Langella, M. Mercurio, G. Soricelli, V. Morra, A Late Roman ceramic production from Pompeii, *J. Archaeol. Sci.* 40 (2013) 810–826. <http://dx.doi.org/10.1016/j.jas.2012.08.043>.
- [5] C. Grifa, L. Cavassa, A. De Bonis, C. Germinario, V. Guarino, F. Izzo, I. Kakoulli, A. Langella, M. Mercurio, V. Morra, Beyond Vitruvius: New Insight in the technology of Egyptian blue and green frits, *J. Am. Ceram. Soc.* 99 (2016) 3467–3475. <http://dx.doi.org/10.1111/jace.14370>.
- [6] A. De Bonis, S. Febbraro, C. Germinario, D. Giampaola, C. Grifa, V. Guarino, A. Langella, V. Morra, Distinctive volcanic material for the production of Campana A Ware: The workshop area of Neapolis at the Duomo Metro Station in Naples, Italy, *Geoarchaeology* 31 (2016) 437–466. <http://dx.doi.org/10.1002/gea.21571>.
- [7] F. Izzo, A. Arizzi, P. Cappelletti, G. Cultrone, A. De Bonis, C. Germinario, S.F. Graziano, C. Grifa, V. Guarino, M. Mercurio, V. Morra, A. Langella, The art of building in the Roman period (89 B.C.–79 A.D.): Mortars, plasters and mosaic floors from ancient Stabiae (Naples, Italy), *Constr. Build. Mater.* 117 (2016) 129–143. <http://dx.doi.org/10.1016/j.conbuildmat.2016.04.101>.
- [8] V. Guarino, A. De Bonis, I. Faga, D. Giampaola, C. Grifa, A. Langella, V. Liuzza, R. Pierobon Benoit, P. Romano, V. Morra, Production and circulation of thin walled pottery from the Roman port of Neapolis, Campania (Italy), *Period. Mineral.* 85 (2016) 95–114. <http://dx.doi.org/10.2451/2016PM618>.
- [9] C. Germinario, G. Cultrone, A. De Bonis, F. Izzo, A. Langella, M. Mercurio, V. Morra, A. Santoriello, S. Siano, C. Grifa, The combined use of spectroscopic techniques for the characterisation of Late Roman common wares from Benevento (Italy), *Measurement* (2016). <http://dx.doi.org/10.1016/j.measurement.2016.08.005>.
- [10] M. de' Gennaro, D. Calcaterra, P. Cappelletti, A. Langella, V. Morra, Building stone and related weathering in the architecture of the ancient city of Naples, *J. Cult. Herit.* 1 (2000) 399–414. [http://dx.doi.org/10.1016/S1296-2074\(00\)01096-7](http://dx.doi.org/10.1016/S1296-2074(00)01096-7).
- [11] V. Morra, D. Calcaterra, P. Cappelletti, A. Colella, L. Fedele, R. de' Gennaro, A. Langella, M. Mercurio, M. de' Gennaro, Urban geology: relationships between geological setting and architectural heritage of the Neapolitan area, in: M. Beltrando, A. Peccerillo, M. Mattei, S. Coticelli, C. Doglioni (Eds.), *The geology of Italy: tectonics and life along plate margins*, *J. Virtual Explor.*, 36, 2010 (<http://dx.doi.org/10.3809/jvirtex.2010.00261>).
- [12] G. Buchner, I giacimenti di argilla dell'isola d'Ischia e l'industria figulina locale in età recente, in: G. Donatone (Ed.) *Quaderno del Centro studi per la storia della ceramica meridionale*, Unigrafica Corcelli, Bari, Italy, 1994, pp. 17–45.
- [13] G. Olcese, Le anfore greco italiche di Ischia: archeologia e archeometria, *Artigianato ed economia nel Golfo di Napoli*, Immensa Aequora 1, Edizioni Quasar, Roma, Italy, 2010.
- [14] A. De Bonis, C. Grifa, G. Cultrone, P. De Vita, A. Langella, V. Morra, Raw materials for archaeological pottery from the Campania Region of Italy: A petrophysical characterization, *Geoarchaeology* 28 (2013) 478–503. <http://dx.doi.org/10.1002/gea.21450>.
- [15] A. De Bonis, G. Cultrone, C. Grifa, A. Langella, V. Morra, Clays from the Bay of Naples (Italy): New insight on ancient and traditional ceramics, *J. Eur. Ceram. Soc.* 34 (2014) 3229–3244. <http://dx.doi.org/10.1016/j.jeurceramsoc.2014.04.014>.
- [16] J. Molera, T. Pradell, M. Vendrell-Saz, The colours of Ca-rich ceramic pastes: origin and characterization, *Appl. Clay Sci.* 13 (1998) 187–202. [http://dx.doi.org/10.1016/S0169-1317\(98\)00024-6](http://dx.doi.org/10.1016/S0169-1317(98)00024-6).
- [17] V. Valanciene, R. Siauciunas, J. Baltusnikaitė, The influence of mineralogical composition on the colour of clay body, *J. Eur. Ceram. Soc.* 30 (2010) 1609–1617. <http://dx.doi.org/10.1016/j.jeurceramsoc.2010.01.017>.
- [18] G. Cultrone, E. Sebastián, Fly ash addition in clayey materials to improve the quality of solid bricks, *Constr. Build. Mater.* 23 (2009) 1178–1184. <http://dx.doi.org/10.1016/j.conbuildmat.2008.07.001>.
- [19] M. Picon, Les modes de cuisson, les pâtes et les vernis de La Graufesenque: une mise au point, in: M. Genin, A. Vernhet (Eds.), *Céramiques de la Graufesenque et autres productions d'époque romaine*, Nouvelles recherches, Hommages à Bettina Hoffmann, Archéologie et Histoire romaine 7, Monique Mergoïl, Montagnac, France, 2002, pp.139–164.
- [20] C. Grifa, A. De Bonis, V. Guarino, C.M. Petrone, C. Germinario, M. Mercurio, G. Soricelli, A. Langella, V. Morra, Thin walled pottery from Alife (Northern Campania, Italy), *Period. Mineral.* 84 (2015) 65–90. <http://dx.doi.org/10.2451/2015PM0005>.
- [21] V. Guarino, A. De Bonis, C. Grifa, A. Langella, V. Morra, L. Pedroni, Archaeometric study on terra sigillata from Cales (Italy), *Period. Mineral.* 80 (2011) 455–470. <http://dx.doi.org/10.2451/2011PM0030>.
- [22] A. De Bonis, C. Grifa, A. Langella, M. Mercurio, M.L. Perrone, V. Morra, Archaeometric study of roman pottery from Caudium area (Southern Italy), *Period. Mineral.* 79 (2010) 73–89. <http://dx.doi.org/10.2451/2010PM0011>.
- [23] G. Cultrone, C. Rodríguez-Navarro, E. Sebastián, O. Cazalla, M.J. de la Torre, Carbonate and silicate phase reactions during ceramic firing, *Eur. J. Mineral.* 13 (2001) 621–634. <http://dx.doi.org/10.1127/0935-1221/2001/0013-0621>.
- [24] C. Grifa, G. Cultrone, A. Langella, M. Mercurio, A. De Bonis, E. Sebastián, V. Morra, Ceramic replicas of archaeological artefacts in Benevento area (Italy): Petrophysical changes induced by different proportions of clays and temper, *Appl. Clay Sci.* 46 (2009) 231–240. <http://dx.doi.org/10.1016/j.clay.2009.08.007>.
- [25] A.P. Leone, Spettrometria e valutazione della riflettanza spettrale dei suoli nel dominio ottico 400–2500 nm, *Riv. Ital. Telerilevamento* 19 (2000) 1–26.
- [26] A.P. Leone, R. Escadafal, Statistical analysis of soil colour and spectroradiometric data for hyperspectral remote sensing of soil properties (example in a southern Italy Mediterranean ecosystem), *Int. J. Remote Sens.* 12 (2001) 2311–2328. <http://dx.doi.org/10.1080/01431160120522>.
- [27] A.P. Leone, R. Viscarra-Rossel, P. Amenta, A. Buondonno, Prediction of soil properties with PLSR and vis-NIR spectroscopy: Application to Mediterranean soils from southern Italy, *Curr. Anal. Chem.* 8 (2012) 283–299. <http://dx.doi.org/10.2174/157341112800392571>.
- [28] F. Bloisi, C. Ebanista, L. Falcone, L. Vicari, Infrared image analysis and elaboration for archaeology: The case study of a medieval “capsella” from Cimitile, Italy, *Appl. Phys. B Lasers Opt.* 101 (2010) 471–479. <http://dx.doi.org/10.1007/s00340-010-4049-z>.
- [29] C. Bonifazzi, P. Carcagni, R. Fontana, M. Greco, M. Mastroianni, M. Materazzi, E. Pampaloni, L. Pezzati, D. Bencini, A scanning device for VIS–NIR multispectral imaging of paintings, *J. Opt. A Pure Appl. Opt.* 10 (64011) (2008) 9. <http://dx.doi.org/10.1088/1464-4258/10/6/064011>.
- [30] P. Vandenabeele, R. Garcia-Moreno, F. Mathis, K. Letermea, E. Van Elslandec, F.P. Hocquet, S. Rakkaa, D. Laboury, L. Moens, D. Strivay, M. Hartwig, Multidisciplinary investigation of the tomb of Menna (TT69), Theban Necropolis, Egypt, *Spectrochim. Acta A* 73 (2009) 546–552. <http://dx.doi.org/10.1016/j.saa.2008.07.028>.
- [31] O. Opuchovic, A. Kareiva, Historical hematite pigment: Synthesis by an aqueous sol-gel method, characterization and application for the colouration of ceramic glazes, *Ceram. Int.* 41 (2015) 4504–4513. <http://dx.doi.org/10.1016/j.ceramint.2014.11.145>.
- [32] M. Sargüzel, Ş. Yılmaz, E. Günay, An investigation of nanoparticles in contemporary lustres on modern Iznik tiles, *J. Aust. Ceram. Soc.* 51 (2015) 34–39.
- [33] P. Mirti, On the use of colour coordinates to evaluate firing temperatures of ancient pottery, *Archaeometry* 40 (1998) 45–57. <http://dx.doi.org/10.1111/j.1475->

- 4754.1998.tb00823.x.
- [34] P. Mirti, P. Davit, New developments in the study of ancient pottery by colour measurement, *J. Archaeol. Sci.* 31 (2004) 741–751. <http://dx.doi.org/10.1016/j.jas.2003.11.006>.
- [35] G. Cultrone, E. Molina, C. Grifa, E. Sebastián, Iberian ceramic production from Basti (Baza, Spain): First geochemical, mineralogical and textural characterization, *Archaeometry* 53 (2011) 340–363. <http://dx.doi.org/10.1111/j.1475-4754.2010.00545.x>.
- [36] A. De Bonis, V. Guarino, L. Sernicola, On some unidentified ceramic objects from Seglamen, Northern Ethiopia, *Rend. Online Soc. Geol. Ital.* 39 (2016) 150–154. <http://dx.doi.org/10.3301/ROL.2015.163>.
- [37] A. De Bonis, M. D'Angelo, V. Guarino, S. Massa, F. Saiedi-Anaraki, B. Genito, V. Morra, Unglazed pottery from the masjed-i jom'e of Isfahan (Iran): technology and provenance, *Archaeol. Anthr. Sci.* (2016). <http://dx.doi.org/10.1007/s12520-016-0407-z>.
- [38] N. Leone, M. Mercurio, E. Grilli, A.P. Leone, A. Langella, A. Buondonno, Potential of vis-NIR reflectance spectroscopy for the mineralogical characterization of synthetic gleys: a preliminary investigation, *Period. Mineral.* 80 (2011) 433–453. <http://dx.doi.org/10.2451/2011PM0029>.
- [39] A. Savitzky, M.J.E. Golay, Smoothing and differentiation of data by simplified least squares procedures, *Anal. Chem.* 36 (1964) 1627–1639. <http://dx.doi.org/10.1021/ac60214a047>.
- [40] G. Calabrò, M. Tosca, SpecPro release a 2.95, Software per il processing di dati spettroradiometrici, Report CNR-ISAFoM, 2009.
- [41] G. Loercher, Investigation of data processing model for integrating hyperspectral data sets into GIS, in: *Proceedings of the Second International Airborne Remote Sensing Conference and Exhibition*, San Francisco, California, 3, 1996, pp. 112–117.
- [42] B. Escofier, J. Pagès, Presentation of correspondence analysis and multiple correspondence analysis with the help of examples, in: J. Devillers, W. Karcher (Eds.), *Applied Multivariate Analysis in SAR and Environmental Studies*, Kluwer Academic Publishers, Dordrecht, the Netherlands, 1991, pp. 1–32.
- [43] A.P. Leone, S. Sommer, Multivariate analysis of laboratory spectra for the assessment of soil development and soil degradation in the Southern Apennines (Italy), *Remote Sens. Environ.* 72 (2000) 346–359. [http://dx.doi.org/10.1016/S0034-4257\(99\)00110-8](http://dx.doi.org/10.1016/S0034-4257(99)00110-8).
- [44] J.F. Hair Jr., R.E. Anderson, R.L. Tatham, W.C. Black, *Multivariate Data Analysis*, Prentice Hall, Englewood Cliffs, New Jersey, USA, 1995.
- [45] C. Rathossi, Y. Pontikes, Effect of firing temperature and atmosphere on ceramics made of NW Peloponnese clay sediments. Part I: Reaction paths, crystalline phases, microstructure and colour, *J. Eur. Ceram. Soc.* 30 (2010) 1841–1851. <http://dx.doi.org/10.1016/j.jeurceramsoc.2010.02.002>.
- [46] L. Nodari, E. Marcuz, L. Maritan, C. Mazzoli, U. Russo, Hematite nucleation and growth in the firing of carbonate-rich clay for pottery production, *J. Eur. Ceram. Soc.* 27 (2007) 4665–4673. <http://dx.doi.org/10.1016/j.jeurceram-soc.2007.03.031>.
- [47] J. Torrent, V. Barrón, Diffuse reflectance spectroscopy of iron oxides, *Encycl. Surf. Colloid Sci.* 1 (2002) 1438–1446.
- [48] M. Maggetti, C. Neururer, D. Ramseyer, Temperature evolution inside a pot during experimental surface (bonfire) firing, *Appl. Clay Sci.* 53 (2011) 500–508. <http://dx.doi.org/10.1016/j.clay.2010.09.013>.
- [49] L. Maritan, L. Nodari, C. Mazzoli, A. Milano, U. Russo, Influence of firing conditions on ceramic products: experimental study on clay rich in organic matter, *Appl. Clay Sci.* 31 (2006) 1–15. <http://dx.doi.org/10.1016/j.clay.2005.08.007>.
- [50] W. Bender, F. Handle, *Brick and Tile Making, Procedures and Operating Practice in the Heavy Clay Industries*, Bauverlag GmbH, Berlin, Germany, 1982.
- [51] K. Pye, *Geological and Soil Evidence: Forensic Applications*, CRC Press, Taylor & Francis Group, Boca Raton, Florida, USA, 2007.
- [52] I.L. Bashar, I. Garba, An overview of VIS-NIR laboratory spectroscopy technique as applied to the analysis of engineering index properties of a geologic material, *Int. J. Sci. Technol. Soc.* 2 (2014) 33–39. <http://dx.doi.org/10.11648/j.ijsts.20140203.11>.
- [53] J.A. de Senna, C.R. de Souza Filho, R.S. Angélica, Characterization of clays used in the ceramic manufacturing industry by reflectance spectroscopy: An experiment in the São Simão ball-clay deposit, Brazil, *Appl. Clay Sci.* 41 (2008) 85–98. <http://dx.doi.org/10.1016/j.clay.2007.10.004>.
- [54] R.A. Viscarra Rossel, R.N. McGlynn, A.B. McBratney, Determining the composition of mineral-organic mixes using UV-vis-NIR diffuse reflectance spectroscopy, *Geoderma* 137 (2006) 70–82. <http://dx.doi.org/10.1016/j.geoderma.2006.07.004>.